

## Strengthening effects evaluation on fatigue damage of rib to deck joint in orthotropic steel deck

Xin, Haohui; Liu, Jieli; Correia, Jose A.F.; Berto, Filippo; Veljkovic, Milan; Yang, Fei

**DOI**

[10.1016/j.engfailanal.2022.107041](https://doi.org/10.1016/j.engfailanal.2022.107041)

**Publication date**

2023

**Document Version**

Final published version

**Published in**

Engineering Failure Analysis

**Citation (APA)**

Xin, H., Liu, J., Correia, J. A. F., Berto, F., Veljkovic, M., & Yang, F. (2023). Strengthening effects evaluation on fatigue damage of rib to deck joint in orthotropic steel deck. *Engineering Failure Analysis*, 145, Article 107041. <https://doi.org/10.1016/j.engfailanal.2022.107041>

**Important note**

To cite this publication, please use the final published version (if applicable). Please check the document version above.

**Copyright**

Other than for strictly personal use, it is not permitted to download, forward or distribute the text or part of it, without the consent of the author(s) and/or copyright holder(s), unless the work is under an open content license such as Creative Commons.

**Takedown policy**

Please contact us and provide details if you believe this document breaches copyrights. We will remove access to the work immediately and investigate your claim.

***Green Open Access added to TU Delft Institutional Repository***

***'You share, we take care!' - Taverne project***

**<https://www.openaccess.nl/en/you-share-we-take-care>**

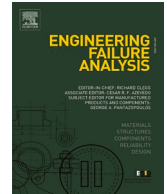
Otherwise as indicated in the copyright section: the publisher is the copyright holder of this work and the author uses the Dutch legislation to make this work public.



ELSEVIER

Contents lists available at ScienceDirect

## Engineering Failure Analysis

journal homepage: [www.elsevier.com/locate/engfailanal](http://www.elsevier.com/locate/engfailanal)

# Strengthening effects evaluation on fatigue damage of rib to deck joint in orthotropic steel deck

Haohui Xin<sup>a</sup>, Jielin Liu<sup>a</sup>, Jose A.F. Correia<sup>a,b</sup>, Filippo Berto<sup>a,c</sup>, Milan Veljkovic<sup>d</sup>,  
Fei Yang<sup>e,f,\*</sup>

<sup>a</sup> Department of Civil Engineering, Xi'an Jiaotong University, Xi'an 710116, China

<sup>b</sup> Construt and Faculty of Engineering, University of Porto, Porto 4200-465, Portugal

<sup>c</sup> Department of Mechanical and Industrial Engineering, Norwegian University of Science and Technology (NTNU), Norway

<sup>d</sup> Department of Structure Engineering, Delft University of Technology, Delft, the Netherlands

<sup>e</sup> Key Laboratory of Old Bridge Inspection and Reinforcement Technology in Transportation Industry, Chang'an University, Xi'an 710061, China

<sup>f</sup> School of Civil Engineering, Chang'an University, Xi'an 710061, China

## ARTICLE INFO

## Keywords:

Orthotropic steel decks (OSDs)  
Rib to deck joint  
Prestressed strengthening method  
Extended finite element method

## ABSTRACT

Strengthening fatigue damage of orthotropic steel decks (OSDs) needs to comprehensively consider the strengthening effect and the dead weight introduced during the strengthening process, especially for OSDs in super large-span bridges or old renovated bridges, where the dead weight cannot be significantly increased during repair and maintenance. This paper proposed a new CFRP prestressed reinforcement method, that does not significantly increase dead weight while effectively inhibiting fatigue crack growth. The strengthening effects of various strengthening methods on the fatigue crack propagation of rib to deck joint in OSDs were compared. Besides, the strengthening effects of different crack sizes were also analyzed. The results showed that the proposed method is effective in reducing fatigue damage at the rib to deck joint in OSDs.

## 1. Introduction

Orthotropic steel decks (OSDs) are widely used in long-span bridge engineering because of their light weight, high strength, and high degree of assembly. However, the fatigue damage of OSDs under repeated vehicle loads is rising, which significantly affects the service life of long-span bridge structures. This issue has attracted wide attention from academia and engineering [1–4].

The fatigue crack positions of the OSD could be divided into five types[5–6], including 1) locating at the rib to deck joints; 2) locating at the rib to diaphragm joints; 3) locating at splicing joints of the longitudinal rib; 4) locating at the deck-diaphragm-rib joints; 5) locating at horizontal butt joint. As shown in Fig. 1, the cracks of rib to deck joints can be further subdivided into four types, namely ① crack initiation at the weld toe and growth along the thickness direction of the flange, ②the crack initiation at the weld root and growth along the thickness direction of the flange, ③the crack initiation at the weld root and growth along the weld, and ④ crack initiation at the weld toe and growth along the thickness direction of the rib.

Since the top flange directly bears the wheel load, the damage type of crack initiation at the weld toe or weld root and propagation along the thickness of the flange is very common. A problem faced by bridge engineering is how to effectively reinforce the cracked OSD without interrupting traffic and causing less damage to the original structure.

\* Corresponding author.

E-mail address: [f.yang@chd.edu.cn](mailto:f.yang@chd.edu.cn) (F. Yang).

<https://doi.org/10.1016/j.engfailanal.2022.107041>

Received 29 August 2022; Received in revised form 26 December 2022; Accepted 28 December 2022

Available online 31 December 2022

1350-6307/© 2022 Elsevier Ltd. All rights reserved.

At present, the fatigue reinforcement methods of the rib to deck joint of the OSDs mainly include local stiffness reinforcement methods and overall stiffness reinforcement methods. The local stiffness reinforcement method increases the local stiffness of the rib to deck joint and slows down fatigue crack propagation by bolting or pasting reinforcement components. Wang et al. [7] studied the cold maintenance reinforcement technology of bonded angle steel. The results showed that the local stress at the cracking position can be reduced by 40.4% and the fatigue damage can be reduced by 79.6%. Liu et al. [8] used L-shaped CFRP to strengthen the fatigue cracking area of the rib to deck joint of the OSD, and the results showed that the fatigue life of the OSD is increased by 3.18 times by this method. Tabata et al. [9] proposed a reinforcement method of bolting U-shaped steel plates between ribs to strengthen the fatigue cracking area of the rib to deck joint. The results showed that this reinforcement method can reduce the stress of the rib to deck joint welding zone by 10%–40%. Guo et al. [10] studied the reinforcement effect of L-shaped GFRP on the fatigue crack at the rib to deck joint. According to the measured equivalent strain amplitude, this reinforcement method can improve the fatigue performance of the welding area.

The overall stiffness strengthening method reduces the stress level and slows down the fatigue crack propagation at the rib to deck joint by increasing the overall stiffness of the OSD. Zhu et al. [11] studied the fatigue strengthening effect of the ultra-high strength concrete UHPC structural layer on the welding details of the rib to deck joint. The results showed that the stress reduction of welding details is as high as 70.9%. Sofia et al. [12] bonded the steel plate to the surface of the OSD to strengthen the cracking area at the rib to deck joint. According to the test results, the stress level of the repaired OSD is significantly reduced. Sofia et al. [13] also used polyurethane and steel plates to reinforce the welding details of the rib to deck joint. Compared with the unreinforced OSD, the transverse stress at the welding details is reduced by 45% to 55%. Wang et al. [14] strengthened the OSD by pasting steel strips on the top surface of the flange and then paving the UHPC structural layer, which has solved the problem that the fatigue resistance of the UHPC bottom surface does not meet the requirements due to penetrating cracks.

The overall or local stiffness reinforcement method slows down fatigue crack propagation by increasing the structures' stiffness. In general, the fatigue crack growth rate of the OSD is inversely proportional to the increase in stiffness. The greater stiffness increase, the smaller the fatigue crack growth rate. The overall stiffness reinforcement method is generally better than the local stiffness reinforcement method. However, for some special bridges (super-long-span bridges, old refurbished bridges, etc.) that cannot significantly increase the self-weight of the structure, the fatigue reinforcement method of OSDs needs to comprehensively consider the reinforcement effect and the self-weight introduced during the reinforcement process. It is required to minimize fatigue crack propagation without significantly increasing the self-weight of the OSD. The overall stiffness reinforcement method introduces a large number of materials, which not only prolongs the fatigue life of the OSD but also significantly increases the self-weight of the OSD, bringing a new burden to the original bridge structure, which is not conducive to the maintenance and reinforcement of super-long-span bridges and old and renovated bridges. Although the local stiffness reinforcement method uses a small amount of reinforcement material, it only slows down the crack propagation and it is difficult to inhibit the fatigue crack propagation.

In addition to the traditional reinforcement method of increasing the stiffness, the method of applying pre-pressure to the cracked area to close the fatigue crack can also improve the fatigue life of the steel structure. Hosseini et al. [15–16] studied the fatigue performance of cracked steel plates strengthened by prestressed CFRP plates, and the results showed that the fatigue crack of the repaired steel plates is arrested. Deng et al. [17] studied the effect of prestressed CFRP on the fatigue strengthening of I-shaped steel beams. The results showed that the fatigue life of repaired steel beams is increased by 7.83 times. This lightweight reinforcement method is suitable for the fatigue reinforcement of OSDs in super-long-span and old refurbished bridges while ensuring excellent fatigue reinforcement effect without significantly increasing the self-weight of the original structure. However, due to the existence of longitudinal ribs, it is impossible to directly arrange the prestressed CFRP plate at the cracked weld toe and weld root like the prestressed reinforcement method of steel beams in reference [17], and there is no reinforcement scheme based on the crack closure principle to strengthen the crack area of the rib to deck joint of the OSD.

Hence, in this paper, a novel lightweight CFRP prestressed reinforcement method was proposed to improve the fatigue performance of the rib to deck joint of the OSD. The fatigue strengthening effects of the proposed CFRP prestressed reinforcement method and the reinforcement method of increasing stiffness were compared using finite element models verified by experiments. The fatigue strengthening effect of the CFRP prestressed reinforcement method on the rib to deck joint of OSDs with different cracking degrees was analyzed.

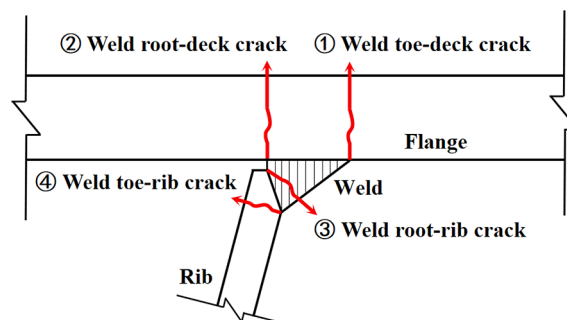


Fig. 1. Schematic diagram of fatigue crack at the position of rib to deck joint.



## 2. Different strengthening methods for rib to deck joints of OSDs

### 2.1. Stiffness increasing reinforcement method

The conventional stiffness reinforcement scheme of the rib to deck joint of the OSD mainly includes the local stiffness reinforcement method and the overall stiffness reinforcement method. The local stiffness reinforcement methods mainly include the steel cover plate reinforcement method, the angle steel reinforcement method, and the CFRP cover plate reinforcement method. As shown in Fig. 2 (a), the steel cover plate reinforcement method refers to welding the steel plate, which is longer than the crack opening length, on the top surface of the flange. By increasing the local stiffness of the section near the crack, the stress intensity factor at the crack tip is reduced, and thus the fatigue life is improved. As shown in Fig. 2 (b), an angle steel with a size larger than the crack opening length is welded or bolted between the bottom of the flange and the U-rib to improve the local rigidity. As shown in Fig. 2 (c), the CFRP cover plate reinforcement method is similar to the steel cover plate reinforcement method. A CFRP plate is bonded on the top surface of the flange to improve the fatigue life.

As shown in Fig. 3, the overall stiffness reinforcement method mainly refers to the use of ultra-high performance concrete (UHPC), the UHPC layer with built-in reinforcement mesh, to be paved on the top surface of the flange to improve the overall stiffness. The UHPC layer and the flange are generally connected by short welding stud.

### 2.2. Crack closure reinforcement method

The crack closure reinforcement scheme can strengthen the OSD by applying pre-pressure to the crack surface to make the fatigue crack close and stop propagation. As shown in Fig. 4, a novel reinforcement scheme is proposed in this paper, which applies tension on both sides on the top of the crack area through prestressed CFRP plates and generates compressive stress on the crack propagation area

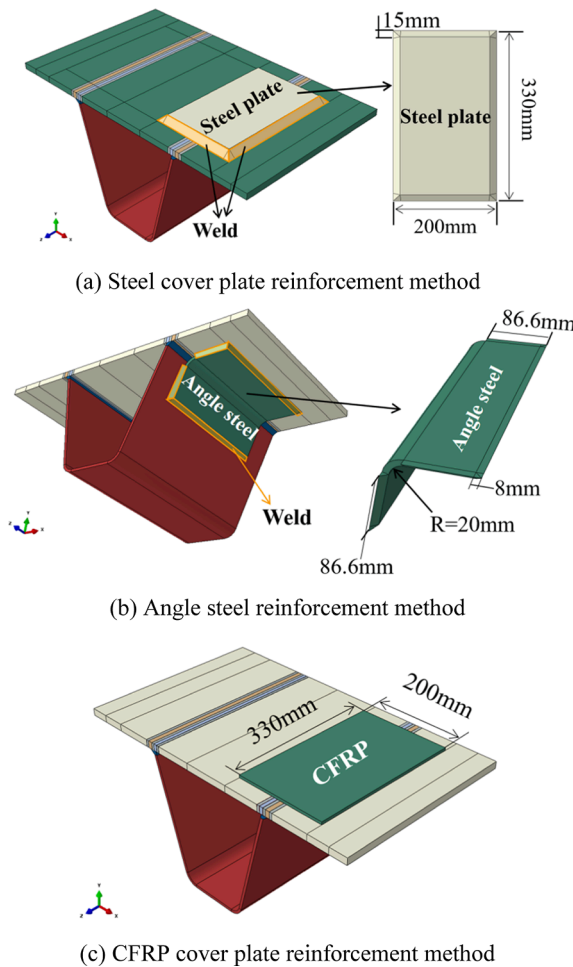


Fig. 2. Conventional local reinforcement method. (a) Steel cover plate reinforcement method (b) Angle steel reinforcement method (c) CFRP cover plate reinforcement method.

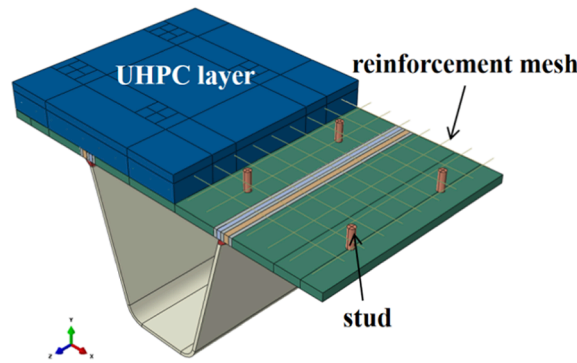


Fig. 3. conventional overall reinforcement method.

through reverse bending moment.

As shown in Fig. 4, the CFRP prestressed reinforcement scheme includes CFRP plates, anchors, and support devices. In the reinforcement process, first a group of anchors are welded on both sides of the top surface of the rib to deck joint, and then the CFRP plate is fixed between the two anchors through high-strength bolts. A support device is arranged between the two anchors and at the bottom of the CFRP plate. The support device includes a support bolt, a support steel plate connected with the support bolt through threads, and a base plate. When the support bolts are rotated at the same time, because the base plate restricts the translational freedom of the support bolt, the support bolts cannot be displaced downward, so the support steel plate and the middle of the CFRP plate are displaced upward, and finally the CFRP plate generates prestress due to extension. The greater the upward displacement of the support plate, the greater the prestress value of CFRP. The relationship between CFRP prestress and displacement can be obtained by experiment, numerical simulation, and geometric analysis. The prestress level of CFRP can be guaranteed by the displacement of the support plate during construction. To prevent fatigue cracks in the welded areas of the anchor and flange, welds can be treated such as by grinding or shot peening. It is noted that local asphalt needs to be removed before installing CFRP prestressed reinforcement devices. After the installation of the reinforcing device is complete, the asphalt layer is poured, and the asphalt layer will wrap the CFRP plate, which is helpful for the durability of the CFRP.

The proposed reinforcement scheme neither requires going deep into the steel box girder for construction nor rewelding the cracked welded joints, so the construction process is relatively simple. Through the above CFRP prestressed reinforcement schemes, the stress intensity factor amplitude of the crack tip of the rib to deck joint of the OSD under the wheel load can be lower than the fatigue threshold, and the fatigue damage of the welding area can be prevented. It has a good application prospect in the bridge system which is sensitive to self-weight, such as super long spans and old renovated bridges.

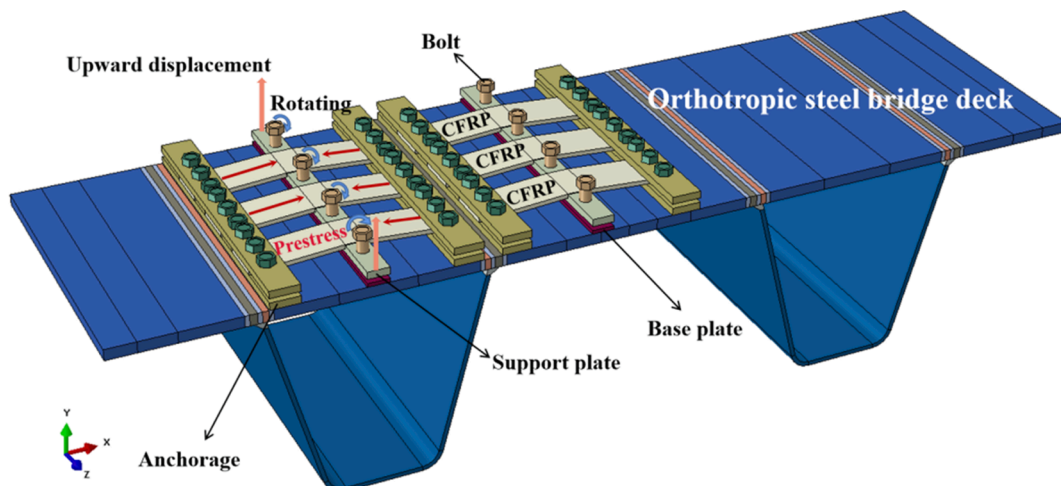


Fig. 4. New CFRP prestressed reinforcement method.

### 3. Validation of the extended finite element model of the OSD

#### 3.1. Fatigue growth test of the OSD

In this paper, the validity of numerical simulation is verified by simulating the fatigue crack propagation test of the rib to deck joint of the OSD [18]. The geometric dimensions and loading condition of the specimen are shown in Figs. 5 and 6. The length of the specimen is 400 mm, the width is 840 mm, and the thickness of the flange is 15 mm; the width of the upper side of the U rib is 300 mm, the width of the lower side is 275 mm, and the thickness is 6 mm. The left end of the specimen is fixed, and the right end is simply supported. A cyclic line load with a maximum load  $P_{max} = 31\text{ kN}$  and a load ratio  $R = 0$  is applied at a distance of 70 mm from the right rib to deck joint. The crack sizes of the specimen were measured using the beach mark technique and fractographic analysis.

#### 3.2. Numerical model and fatigue crack growth rate

The numerical model and its boundary conditions are shown in Fig. 7. The upper and lower sides of the 40 mm area at the left end of the flange are set to fixed constraints, and the lower side of the 50 mm area at the right end is set to Y-direction support. The cyclic line load was applied at a distance of 70 mm from the welded joint. According to the test results, a pre-crack of 275 mm long and 1.5 mm high was inserted in the middle of the weld toe. The elastic modulus and Poisson’s ratio of the OSD are 210 GPa and 0.3, respectively. The element type of the fatigue crack propagation region is C3D8, and the element type of the non-propagation region is set to C3D8R. The mesh in the crack propagation area is encrypted, and the mesh size along the crack propagation direction is 0.75 mm.

The fatigue crack propagation of the OSD is simulated by the extended finite element method (XFEM) [19] based on the phantom node method [20] and virtual crack closure technique (VCCT) [21]. The phantom node method realizes the numerical simulation of fatigue cracks by defining a set of virtual nodes. The VCCT is used to calculate the strain energy release rate of the crack front, and then the stress intensity factor can be obtained based on the fracture mechanics theory. Based on the commercial software ABAQUS and the user-defined subroutine “UMIXMODEFATIGUE”, the numerical simulation of fatigue crack propagation is finally realized [19].

Paris law is used to calculate the fatigue crack growth rate, as shown in Eq. (1). Referring to IIW [22–23], the material parameter  $m$  of the fatigue crack growth rate is 3.0, the median of  $C_0$  is  $2.63 \times 10^{-13}$ , and the discrete coefficient of  $C_0$  is 0.6066. According to the lognormal distribution, the values of material parameter  $C_0$  of fatigue crack growth rate with 95% and 99% guarantee rates are shown in Table 1.

$$\frac{da}{dN} = C_0(\Delta K)^m \tag{1}$$

Where  $\frac{da}{dN}$  is the fatigue crack growth rate.  $C_0$  and  $m$  are the material parameters of the fatigue crack growth rate.  $\Delta K$  is the stress intensity factor amplitude.

#### 3.3. Verification of numerical simulation results of fatigue crack growth

Fig. 8 compares the experimental results with the numerical simulation results. Fig. 9 shows the fatigue crack propagation process. In terms of fatigue crack propagation depth  $a$ , the numerical simulation results are in good agreement with the test data, but the experimental results are slightly larger than the numerical simulation results. In terms of fatigue crack growth width  $2C$ , numerical simulation results are in good agreement with test data. The test data almost falls into the confidence interval with a 95% guarantee rate, indicating that the numerical simulation can reflect the actual fatigue crack propagation process.

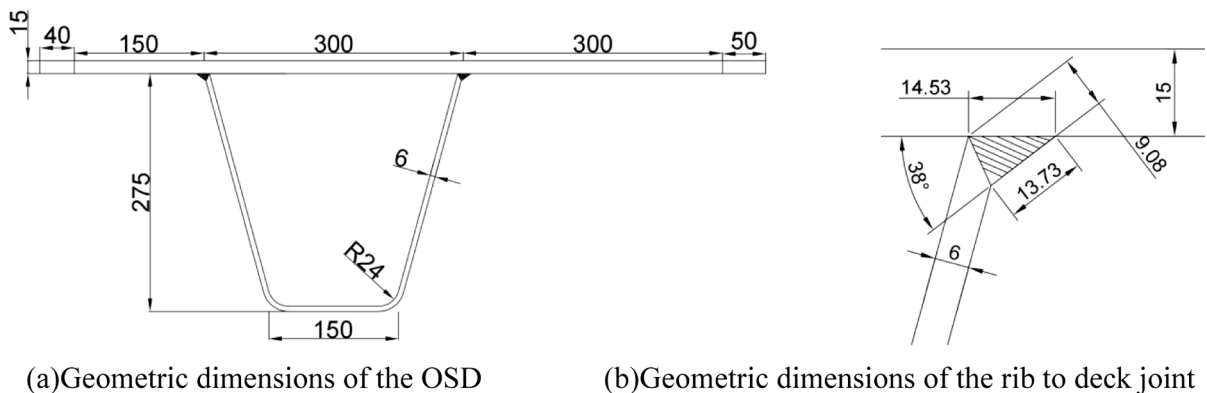


Fig. 5. Geometric dimension of the specimen [18]. (a)Geometric dimensions of the OSD (b)Geometric dimensions of the rib to deck joint.

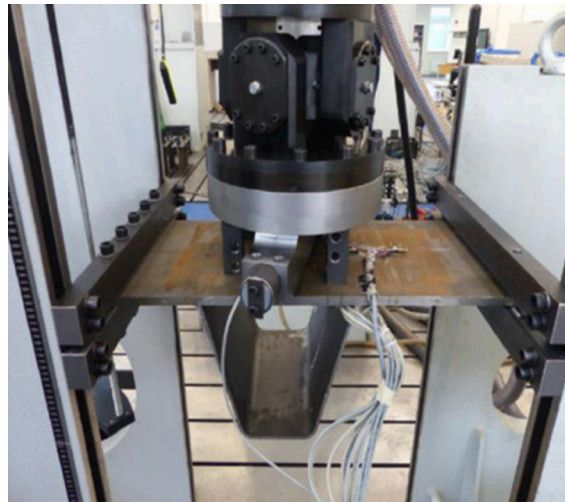


Fig. 6. The loading device for the OSD specimen [18].

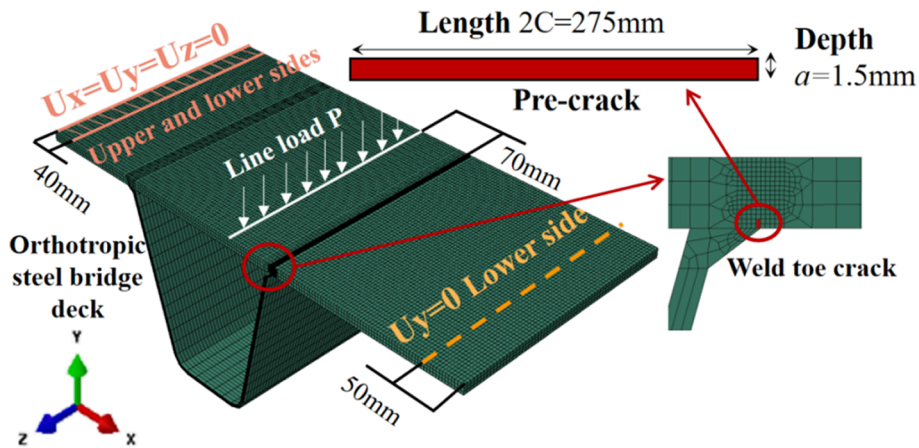


Fig. 7. The numerical model and its boundary conditions.

**Table 1**  
Material coefficient of fatigue crack propagation rate of S355 steel.

|       | Median                 | 95% guarantee rate     |                        | 99% guarantee rate     |                        |
|-------|------------------------|------------------------|------------------------|------------------------|------------------------|
|       |                        | Upper limit            | Lower limit            | Upper limit            | Lower limit            |
| $C_0$ | $2.63 \times 10^{-13}$ | $6.73 \times 10^{-13}$ | $0.75 \times 10^{-13}$ | $9.51 \times 10^{-13}$ | $0.53 \times 10^{-13}$ |
| $m$   | 3.00                   |                        |                        |                        |                        |

#### 4. Reinforcement effects comparison of different methods

##### 4.1. Numerical models of different reinforcement methods

Fig. 10 shows the reference model (not reinforcement) of the OSD. A cyclic loading is applied at a distance of 70 mm from the right rib to deck joint. The types of fatigue crack propagation include cracks initiated at the weld toe and weld root propagated along the thickness direction of the flange. For the numerical model of a crack initiated at the weld toe and propagated along the thickness direction of the flange, the maximum  $P_{max} = 60\text{kN}$  and the load ratio  $R = 0$ . For the numerical model of a crack initiated at the weld root and propagated along the thickness direction of the flange, the maximum  $P_{max} = 100\text{kN}$  and the load ratio  $R = 0$ . The pre-crack length is 200 mm and the height is 1 mm.

By establishing the reinforcement device in the reference model, the numerical models of different reinforcement methods are obtained. The numerical model of the steel cover plate reinforcement method is shown in Fig. 2 (a). The thickness of the steel plate, the

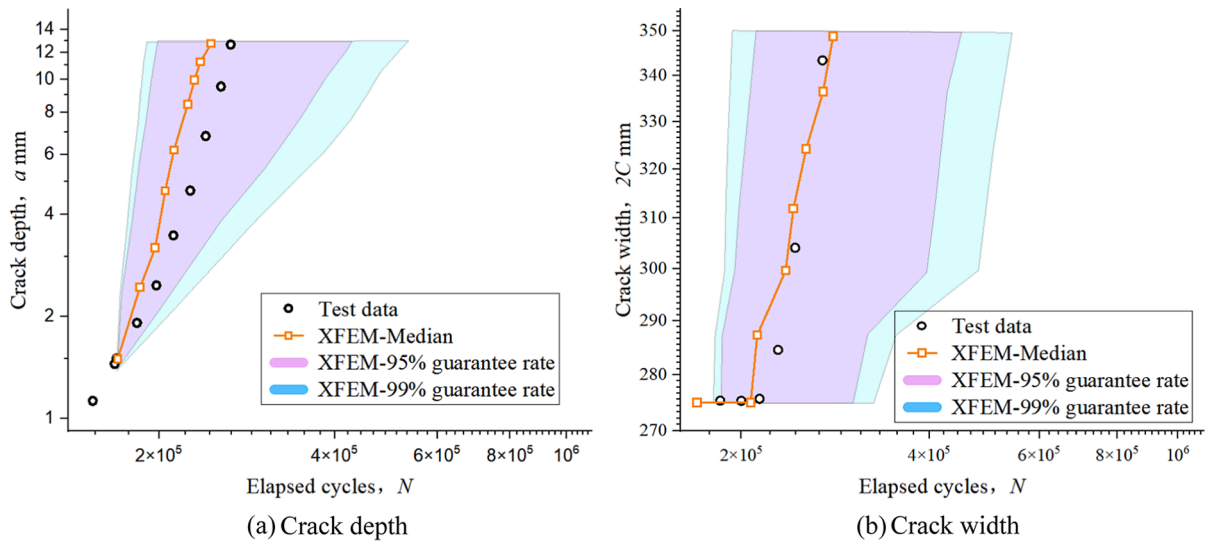


Fig. 8. Test data and numerical simulation results (a)Crack depth (b)Crack width.

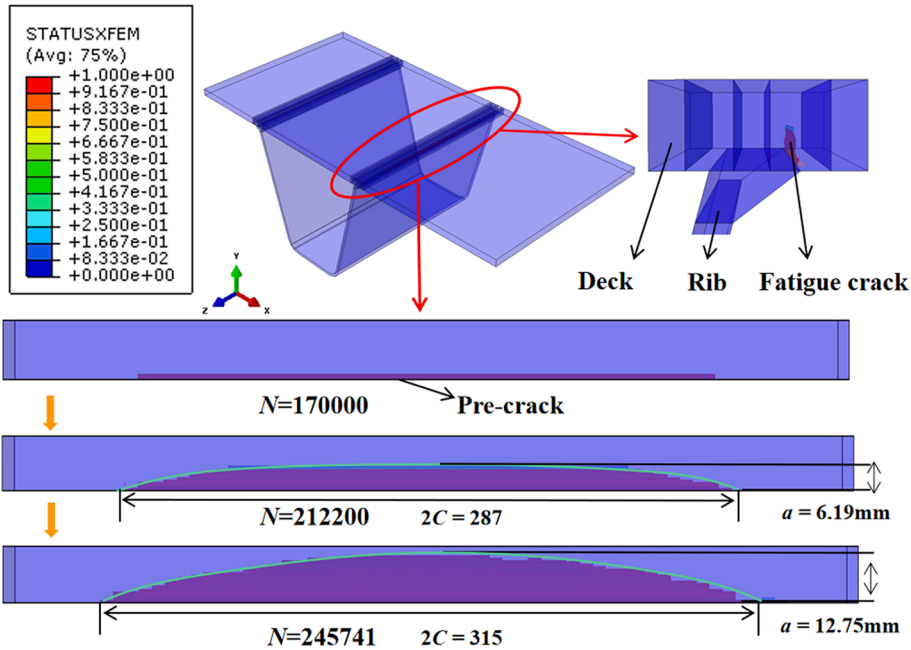


Fig. 9. The fatigue crack growth process of the OSD.

height of the fillet weld, and the width of the weld toe are all 15 mm, and the length and width of the steel plate are 330 mm and 200 mm, respectively. The weld is fixed on flange by Tie restraints, and the hard contact is set between the steel plate and the flange. The numerical model of the angle steel reinforcement method is shown in Fig. 2 (b), where the thickness of angle steel is 8 mm and the welding or bolt connection is simulated by tie constraint. The numerical model of the CFRP plate reinforcement method is shown in Fig. 2 (c). The length, width, and thickness of CFRP plate are 330 mm, 200 mm, and 6 mm, respectively. The type of CFRP is S&P 150/2000, and the mechanical properties are shown in Table 2. The lower surface of the CFRP plate is bound to the flange by the Tie constraint.

The numerical model of the overall stiffness reinforcement method is shown in Fig. 3. The thickness of the UHPC layer is 50 mm, the element mesh type is C3D8R, and the elastic modulus and Poisson’s ratio are 45.56 GPa and 0.2, respectively [24]. The diameter of the steel grid is 10 mm, the interval is 30 mm, the thickness of the protective layer is 15 mm, and the element type is T3D2. The diameter of the stud is 13 mm, the height is 35 mm, and the element type is C3D8R. The steel bar and the stud have the same elastic modulus as the OSD; the Tie constraint connects the UHPC layer, stud, steel bar, and flange.



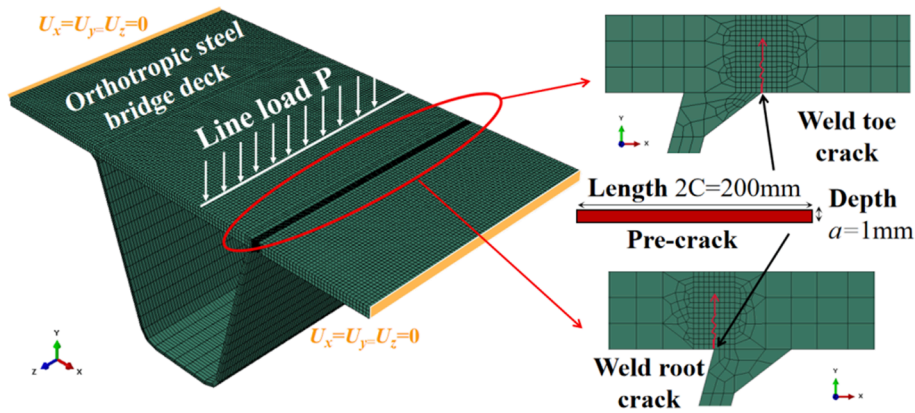


Fig. 10. The finite element model of the unreinforced OSD.

**Table 2**  
The CFRP material properties.

| Longitudinal modulus of elasticity | Transverse modulus of elasticity | Longitudinal Poisson's ratio | Longitudinal shear modulus | Transverse shear modulus | Minimum tensile strength |
|------------------------------------|----------------------------------|------------------------------|----------------------------|--------------------------|--------------------------|
| 156000.00 MPa                      | 40925.00 MPa                     | 0.25                         | 13145.68 MPa               | 13145.68 MPa             | 2800.00 MPa              |

The numerical model of the CFRP prestressed reinforcement scheme is shown in Fig. 11. The geometric dimension of the anchor is  $400\text{ mm} \times 25\text{ mm} \times 15\text{ mm}$ . The geometric dimension of the CFRP plate is  $176.22\text{ mm} \times 30\text{ mm} \times 4\text{ mm}$ . The geometric dimension of the base plate is  $400\text{ mm} \times 25\text{ mm} \times 5\text{ mm}$ . The geometric dimension of the support plate is  $400\text{ mm} \times 25\text{ mm} \times 5\text{ mm}$ . Bolt diameter is 10 mm. In the numerical model, there are Tie constraints between the four anchors and the bridge deck to simulate the welding connection. In the actual design of the construction scheme, both ends of CFRP are fixed by bolts and anchors, so the interface of the CFRP plates and anchors are also Tie constraints. The prestressing device includes a base plate, a support plate, and bolts. Tie constraint is set between the base plate and the bridge deck. The base plate and the support plate form a whole through bolts. Tie constraint is set on the contact surface between the three components. By increasing the temperature of the screw of the bolt, the support plate is displaced upward, and prestressing is introduced into the CFRP plate. The properties of CFRP materials are also shown in Table 2. The relationship between several groups of displacements and CFRP prestress was determined by numerical simulation results. The displacement of the support plate and the prestress of the CFRP plate are shown in Table 3.

Table 4 summarizes the mass of the OSD after reinforcement. Among them, compared with the unreinforced OSD, the weight gain of the CFRP cover plate reinforcement scheme is the smallest, only increasing by 2%. The weight gain of the UHPC overall reinforcement scheme was the highest, increasing by 87%. The weight gain of the CFRP prestressed reinforcement scheme proposed in this paper is 13%, which is between the steel cover plate and the CFRP cover plate reinforcement scheme.

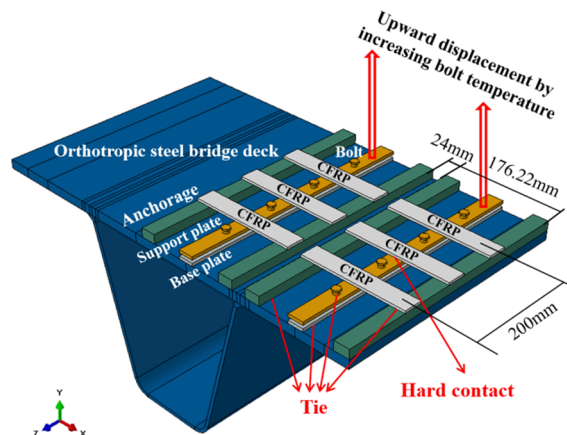


Fig. 11. The numerical model of the CFRP prestressed reinforcement scheme.

**Table 3**  
The level of prestress in the CFRP prestressed strengthening scheme.

| Cracked area | displacement (mm) | Prestress (MPa) |
|--------------|-------------------|-----------------|
| Weld toe     | 0.02              | 0.01            |
|              | 3.40              | 280             |
| Weld root    | 0.02              | 0.01            |
|              | 3.40              | 280             |
|              | 4.80              | 560             |

**Table 4**  
The mass of the OSD using different reinforcement methods.

| Reinforcement scheme                      | Steel plate | Angle steel | CFRP plate | UHPC layer |           | CFRP prestressed |      |
|---|-------------|-------------|------------|------------|-----------|------------------|------|
| Components                                | Steel plate | Angle steel | CFRP plate | UHPC       | steel bar | stud             | CFRP |
| Density (Kg/m <sup>3</sup> )              | 7850        | 7850        | 1800       | 2600       | 7850      | 1800             | 7850 |
| Reinforcement mass (Kg)                   | 7.77        | 3.97        | 0.71       | 39.44      |           | 5.71             |      |
| Total mass (Kg)                           | 53.08       | 49.28       | 46.02      | 84.75      |           | 51.02            |      |
| Mass ratio<br>(reinforced/not reinforced) | 1.17        | 1.09        | 1.02       | 1.87       |           | 1.13             |      |

#### 4.2. Comparison of the strengthening effect of weld toe

Fig. 12 compares the reinforcement effects of different reinforcement methods on weld toes. When the fatigue crack at the weld toe propagates along the flange to the same depth or width, the ratio of fatigue life of the reinforced OSDs to that of the unreinforced OSD is shown in Table 5 and Table 6. In general, the reinforcement effect of the overall stiffness reinforcement method on fatigue cracking at the weld toe is better than that of the local stiffness reinforcement method. When the fatigue crack at weld toe propagates to the same depth, the average fatigue life of the OSD reinforced by the UHPC layer is 626.63 times that of the reference model. When the fatigue crack at the weld toe propagates to the same width, the average fatigue life of the OSD strengthened with the UHPC layer is 392.7 times that of the reference model.

In the local stiffness reinforcement method, the reinforcement effect of the steel cover plate reinforcement method is better than that of the angle steel reinforcement method and the CFRP cover plate reinforcement method. When the fatigue crack at the weld toe propagates to the same depth, the average fatigue life of the OSD reinforced by steel cover plate, angle steel, and CFRP cover plate is 4.30, 1.92, and 1.75 times that of the reference model, respectively. When the fatigue crack at weld toe propagates to the same width, the average fatigue life of the OSD strengthened with steel cover plate, angle steel, and CFRP cover plate is 4.43 times, 1.93 times, and 1.82 times that of the reference model, respectively.

The reinforcement effect of the CFRP prestressed reinforcement method on fatigue cracking at weld toe is better than that of the overall stiffness reinforcement method. When the fatigue crack at the weld toe propagates to the same depth, the average fatigue life of the OSD strengthened with 0.01 MPa prestressed CFRP plate is 4.22 times that of the reference model. When the fatigue crack propagates to the same width, the average fatigue life of the OSD strengthened with 0.01 MPa prestressed CFRP plate is 3.54 times that of the reference model. When the prestress of CFRP plate increases to 280 MPa, the fatigue crack at the weld toe is closed, and the fatigue crack no longer propagates.

Fig. 13 compares the fatigue cracks at the weld toe of different reinforcement models after 1 million cycles of loading. Compared with the reference model, the fatigue cracks of the local reinforcement method have obvious propagation, and the fatigue crack propagation rate of the OSD reinforced with CFRP cover plate is the fastest. The fatigue load is assumed to be 60 kN in this paper. However, there are many heavy-duty vehicles during bridge service. With the increase in load, the propagation speed of fatigue cracks will also increase significantly. The local stiffness reinforcement method cannot completely inhibit the occurrence of fatigue cracks. The fatigue damage of the OSD strengthened with a UHPC layer or prestressed CFRP can be ignored.

Fig. 14 shows the ratio of the average fatigue life ratio to the mass ratio of the reinforced OSD to analyze the comprehensive reinforcement effect. The local stiffness reinforcement method and the proposed CFRP prestressed reinforcement method have little influence on the comprehensive reinforcement effect due to the light weight of reinforcement devices. After considering the self-weight of the reinforcement scheme, the reinforcement effect of 280 MPa prestressed CFRP plates is significantly better than that of the UHPC layer reinforcement method.

#### 4.3. Comparison of the strengthening effect of weld root

Fig. 15 compares the reinforcement effects of different reinforcement methods on weld root. When the fatigue crack at the weld root propagates to the same depth or width, the ratio of fatigue life of the reinforced OSDs to that of the unreinforced OSD is shown in Table 7 and Table 8. The reinforcement effect of the overall stiffness reinforcement method on the fatigue crack at the weld root is still significantly better than that of the local stiffness reinforcement method. When the fatigue crack propagates to the same depth, the average fatigue life of the OSD strengthened with the UHPC layer is 106.95 times that of the reference model. When the fatigue crack at

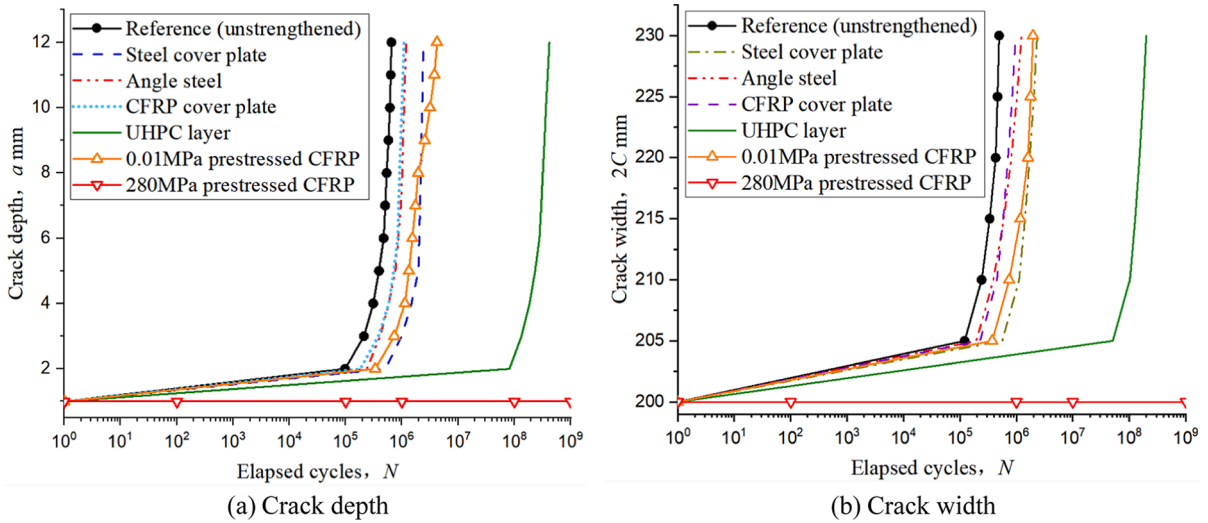


Fig. 12. Numerical simulation results of welded toe fatigue crack propagation. (a)Crack depth (b)Crack width.

Table 5  
Fatigue crack propagation life ratio of welded toe (crack depth).

| Reinforcement scheme | Steel plate | Angle steel | CFRP plate | UHPC layer | 0.01 MPa CFRP prestressed | 280 MPa CFRP prestressed |          |
|----------------------|-------------|-------------|------------|------------|---------------------------|--------------------------|----------|
| Crack depth $a$ (mm) | 1           | NAN         | NAN        | NAN        | NAN                       | NAN                      | NAN      |
|                      | 2           | 5.18        | 2.43       | 1.86       | 832.82                    | 3.44                     | $\infty$ |
|                      | 3           | 4.70        | 1.94       | 1.82       | 633.72                    | 3.46                     | $\infty$ |
|                      | 4           | 4.76        | 1.87       | 1.89       | 601.08                    | 3.63                     | $\infty$ |
|                      | 5           | 5.01        | 1.96       | 1.82       | 596.86                    | 3.40                     | $\infty$ |
|                      | 6           | 4.31        | 1.83       | 1.78       | 594.09                    | 3.26                     | $\infty$ |
|                      | 7           | 4.19        | 1.90       | 1.74       | 595.27                    | 3.46                     | $\infty$ |
|                      | 8           | 4.05        | 1.88       | 1.70       | 596.31                    | 3.64                     | $\infty$ |
|                      | 9           | 3.89        | 1.84       | 1.66       | 594.69                    | 4.47                     | $\infty$ |
|                      | 10          | 3.76        | 1.78       | 1.64       | 593.27                    | 5.20                     | $\infty$ |
|                      | 11          | 3.73        | 1.81       | 1.65       | 615.58                    | 5.99                     | $\infty$ |
|                      | 12          | 3.73        | 1.84       | 1.68       | 639.25                    | 6.45                     | $\infty$ |
| Mean value           | 4.30        | 1.92        | 1.75       | 626.63     | 4.22                      | $\infty$                 |          |

Table 6  
Fatigue crack propagation life ratio of welded toe (crack width).

| Reinforcement scheme | Steel plate | Angle steel | CFRP plate | UHPC layer | 0.01 MPa CFRP prestressed | 280 MPa CFRP prestressed |
|----------------------|-------------|-------------|------------|------------|---------------------------|--------------------------|
| Crack width          | 200         | NAN         | NAN        | NAN        | NAN                       | NAN                      |
| 2C                   | 205         | 4.62        | 1.60       | 1.86       | 422.08                    | 3.07                     |
| (mm)                 | 210         | 4.62        | 1.60       | 1.86       | 422.08                    | 3.07                     |
|                      | 215         | 4.23        | 1.79       | 1.73       | 377.06                    | 3.50                     |
|                      | 220         | 4.01        | 1.89       | 1.66       | 351.64                    | 3.74                     |
|                      | 225         | 4.38        | 2.22       | 1.82       | 379.56                    | 3.86                     |
|                      | 230         | 4.70        | 2.50       | 1.96       | 403.80                    | 3.96                     |
| Mean value           | 4.43        | 1.93        | 1.82       | 392.70     | 3.54                      | $\infty$                 |

the weld root extends to the same width, the average fatigue life of the OSD strengthened with the UHPC layer is 133.69 times that of the reference model.

In the local stiffness reinforcement method, the reinforcement effect of the steel cover plate reinforcement method is still better than that of the angle steel and CFRP cover plate reinforcement methods. When the fatigue crack propagates to the same depth, the average fatigue life of the OSD strengthened with the steel cover plate, angle steel, and CFRP cover plate is 3.43, 1.03, and 1.61 times that of the reference model, respectively. When the fatigue crack at the weld root propagates to the same width, the average fatigue life of the OSD strengthened with the steel cover plate, angle steel, and CFRP cover plate is 6.30, 2.36, and 1.79 times that of the reference model, respectively.

The reinforcement effect of the CFRP prestressed reinforcement method on the weld root is related to the prestress level of the CFRP plates. When the prestress level is low, the reinforcement effect of the CFRP prestressed reinforcement method is not as good as that of



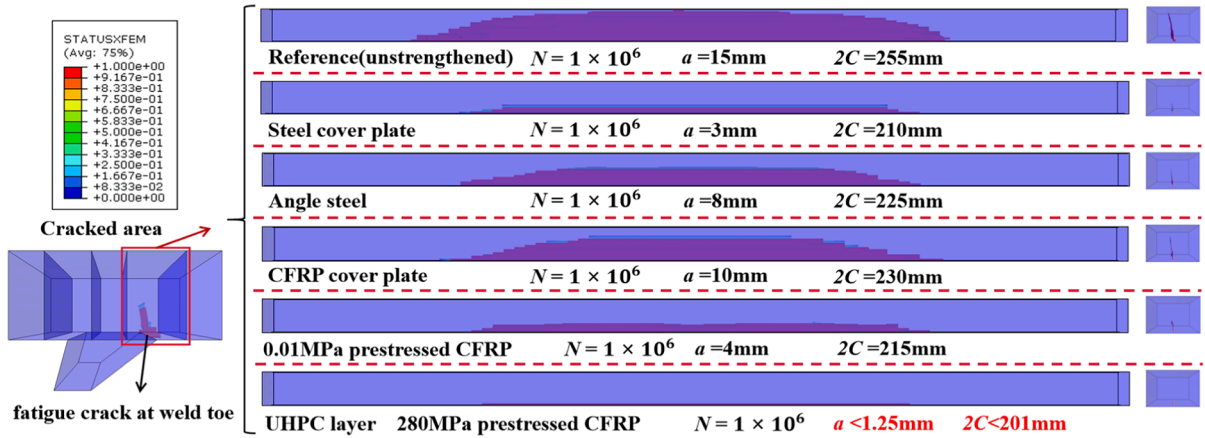


Fig. 13. Fatigue crack at welded toe after  $1 \times 10^6$  cycle loads.

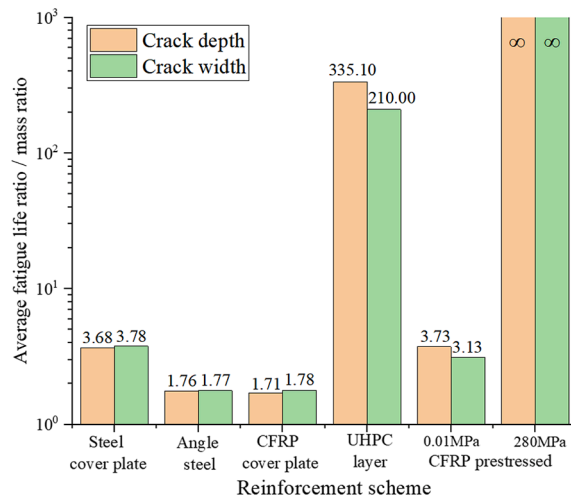


Fig. 14. Comprehensive fatigue reinforcement effect at welded toe considering self-weight of reinforcement scheme.

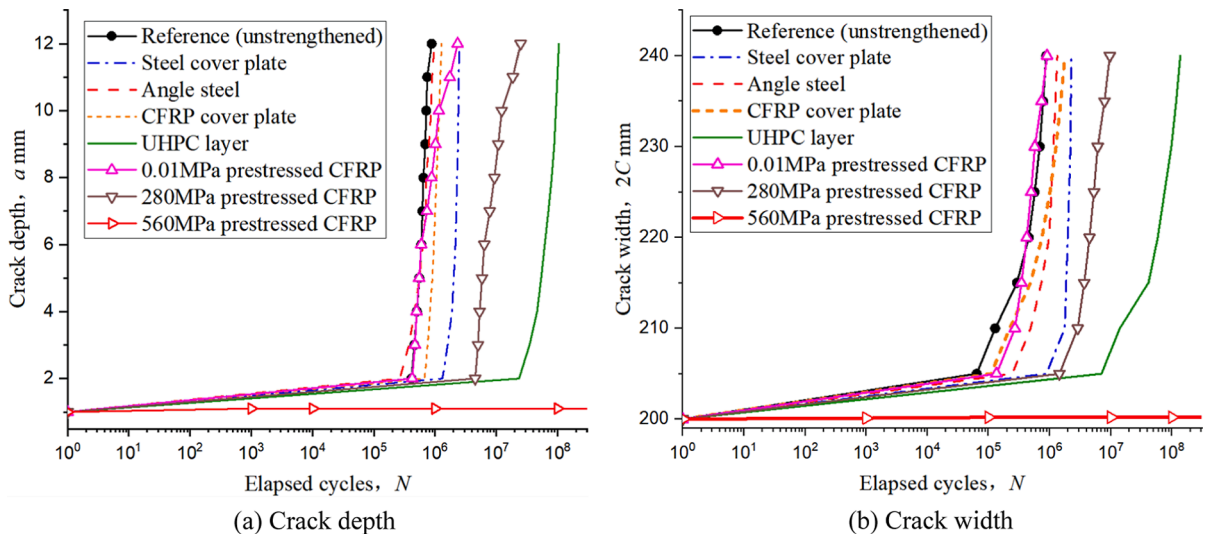


Fig. 15. Numerical simulation results of welded root fatigue crack propagation. (a)Crack depth (b)Crack width.

**Table 7**  
Fatigue crack propagation life ratio of welded root (Crack depth).

| Reinforcement scheme | Steel plate | Angle steel | CFRP plate | UHPC layer | 0.01 MPa CFRP prestressed | 280 MPa CFRP prestressed | 560 MPa CFRP prestressed |
|----------------------|-------------|-------------|------------|------------|---------------------------|--------------------------|--------------------------|
| Crack depth          | 1           | NAN         | NAN        | NAN        | NAN                       | NAN                      | NAN                      |
| <i>a</i>             | 2           | 3.19        | 0.64       | 1.63       | 56.47                     | 1.02                     | 10.91                    |
| (mm)                 | 3           | 3.49        | 0.82       | 1.64       | 75.71                     | 1.03                     | 10.92                    |
|                      | 4           | 3.75        | 0.92       | 1.64       | 91.48                     | 0.99                     | 10.57                    |
|                      | 5           | 3.68        | 1.01       | 1.64       | 98.02                     | 1.00                     | 10.61                    |
|                      | 6           | 3.62        | 1.05       | 1.60       | 103.56                    | 1.00                     | 10.65                    |
|                      | 7           | 3.58        | 1.13       | 1.62       | 114.29                    | 1.18                     | 12.62                    |
|                      | 8           | 3.55        | 1.11       | 1.64       | 124.21                    | 1.36                     | 14.44                    |
|                      | 9           | 3.43        | 1.15       | 1.61       | 128.32                    | 1.47                     | 15.67                    |
|                      | 10          | 3.35        | 1.21       | 1.62       | 131.22                    | 1.61                     | 17.14                    |
|                      | 11          | 3.29        | 1.20       | 1.64       | 133.90                    | 2.35                     | 25.03                    |
|                      | 12          | 2.83        | 1.11       | 1.44       | 119.30                    | 2.66                     | 28.31                    |
| Mean value           | 3.43        | 1.03        | 1.61       | 106.95     | 1.42                      | 15.17                    | ∞                        |

**Table 8**  
Fatigue crack propagation life ratio of welded root (Crack width).

| Reinforcement scheme | Steel plate | Angle steel | CFRP plate | UHPC layer | 0.01 MPa CFRP prestressed | 280 MPa CFRP prestressed | 560 MPa CFRP prestressed |
|----------------------|-------------|-------------|------------|------------|---------------------------|--------------------------|--------------------------|
| Crack width          | 200         | NAN         | NAN        | NAN        | NAN                       | NAN                      | NAN                      |
| <i>2C</i>            | 205         | 13.72       | 3.80       | 1.72       | 109.44                    | 2.10                     | 22.41                    |
| (mm)                 | 210         | 13.72       | 3.80       | 1.72       | 109.44                    | 2.10                     | 22.41                    |
|                      | 215         | 6.41        | 2.52       | 1.67       | 141.76                    | 1.19                     | 12.65                    |
|                      | 220         | 4.34        | 2.15       | 1.66       | 128.65                    | 0.93                     | 9.89                     |
|                      | 225         | 3.64        | 1.87       | 1.77       | 132.38                    | 0.87                     | 9.29                     |
|                      | 230         | 3.18        | 1.68       | 1.84       | 142.19                    | 0.83                     | 8.89                     |
|                      | 235         | 2.83        | 1.58       | 1.94       | 149.85                    | 0.94                     | 10.04                    |
|                      | 240         | 2.56        | 1.51       | 2.02       | 155.83                    | 1.03                     | 10.95                    |
| Mean value           | 6.30        | 2.36        | 1.79       | 133.69     | 1.25                      | 13.32                    | ∞                        |

the overall stiffness reinforcement method. When the prestress level increases to the crack tip completely closed, the reinforcement effect of the CFRP prestressed reinforcement method is better than that of the overall stiffness reinforcement method. The average fatigue life of the OSDs strengthened with 0.01 MPa and 280.0 MPa prestressed CFRP plates is 1.42 and 15.17 times that of the reference model when the fatigue crack at the weld root propagates to the same depth. When the fatigue crack at the weld root propagates to the same width, the average fatigue life of the OSDs strengthened with 0.01 MPa and 280.0 MPa prestressed CFRP plates is 1.25 and 13.32 times that of the reference model. When the prestress of CFRP plate increases to 560.0 MPa, the fatigue crack at the weld root is closed, and the fatigue crack no longer propagates.

Fig. 16 compares the fatigue cracks at the weld root of different reinforcement models after 1 million cycles of loading. In the local stiffness reinforcement method, the fatigue damage of OSDs reinforced by steel cover plate is small, while the OSDs reinforced by angle steel have significant fatigue damage, and the crack depth has reached 12 mm. The reinforcement effect of 0.01 MPa CFRP plates is not

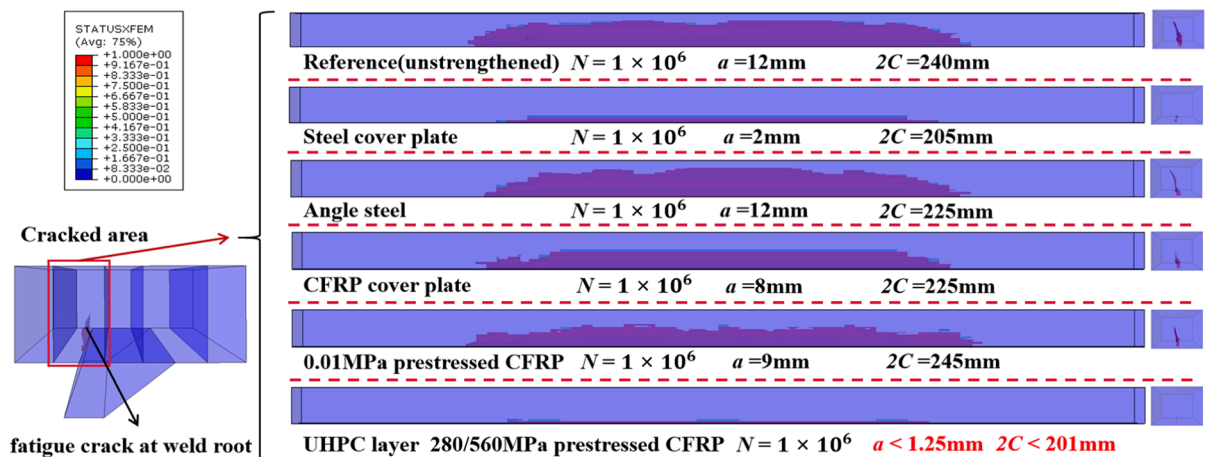


Fig. 16. Fatigue crack at welded root after  $1 \times 10^6$  cycle loads.

ideal. The fatigue damage to the OSDs reinforced with the UHPC layer, 280.0 MPa and 560.0 MPa prestressed CFRP plates is minor.

Fig. 17 compares the comprehensive reinforcement effects of different reinforcement schemes on the weld root. Due to the influence of the UHPC layer mass, the comprehensive reinforcement effect is weakened. However, compared with the local stiffness reinforcement method, the comprehensive reinforcement effect of the UHPC reinforcement method still has a very significant advantage. When the prestress of CFRP plate is greater than 560.0 MPa, the comprehensive reinforcement effect of prestress is the best.

### 5. The strengthening effect on OSDs with different crack size

Fig. 18 is the numerical model of the OSD strengthened with prestressed CFRP plate considering different pre-crack heights. The geometric dimensions of pre-cracks with a height of 5 mm, 10 mm, and 15 mm are determined according to the fatigue crack growth simulation results of the reference model. For the fatigue crack propagation numerical model of weld toe, the prestress of the CFRP plate is 280.0 MPa. For the fatigue crack propagation numerical model of weld root, the prestress of the CFRP plate is 560.0 MPa. See Section 4.1 for load and boundary conditions.

Fig. 19 compares the simulation results of fatigue crack propagation along the depth direction between the reference model and the CFRP prestressed reinforcement model. When the pre-crack height is 5 mm or 10 mm, the fatigue crack at the weld toe of the CFRP prestressed reinforcement model stops propagating. When the height of the pre-crack is 5 mm, the fatigue crack at the weld root of the CFRP prestressed reinforcement model stops propagation. When the pre-crack height is 10 mm, the fatigue crack at the weld root propagates along the depth direction, and the average fatigue life is 107.01 times that of the reference model (see Table 9).

Fig. 20 compares the simulation results of fatigue crack propagation along the width direction between the reference model and the CFRP prestressed reinforcement model. When the pre-crack height is 5 mm, 10 mm, or 15 mm, the fatigue crack at the weld toe of the CFRP prestressed reinforcement model stops propagation. When the height of the pre-crack is 5 mm or 10 mm, the fatigue crack at the weld root of the CFRP prestressed reinforcement model stops propagation. When the pre-crack height is 15 mm, the fatigue crack at the weld root propagates along the width direction, and the average fatigue life is 40.41 times that of the reference model (see Table 10).

### 6. Conclusion

In this paper, a new CFRP prestressed reinforcement method was proposed to strengthen the rib to deck joint of the OSD, which does not significantly increase the dead weight and can effectively inhibit the growth of fatigue cracks. Based on the extended finite element model checked by experiment, the fatigue strengthening effects of different methods on the fatigue cracking of the rib to deck joint of the OSD were compared. The following conclusions are obtained:

1. The reinforcement effect of the overall stiffness reinforcement scheme is significantly better than that of the local stiffness reinforcement scheme. The self-weight of the OSD strengthened with the UHPC layer increases by 87%, the average fatigue life of fatigue cracking at weld toe increases by 625 times, and the average fatigue life of fatigue cracking at weld root increases by 105 times.
2. In the local stiffness reinforcement scheme, the steel cover plate reinforcement method has the best reinforcement effect on the weld toe or weld root. After increasing the self-weight by 17%, the average fatigue life of the cracked weld toe is increased by 3.3 times, and the average fatigue life of the cracked weld root is increased by 2.43 times by using the steel cover plate reinforcement scheme. The CFRP cover plate reinforcement scheme only increases the self-weight of the OSD by 2%, increases the average fatigue life of the weld toe by 0.75 times, and increases the average fatigue life of the weld root by 0.61 times.

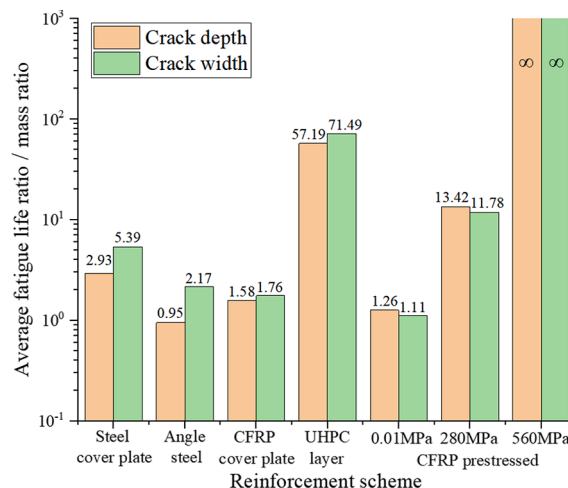


Fig. 17. Comprehensive fatigue reinforcement effect at welded root considering self-weight of reinforcement scheme.

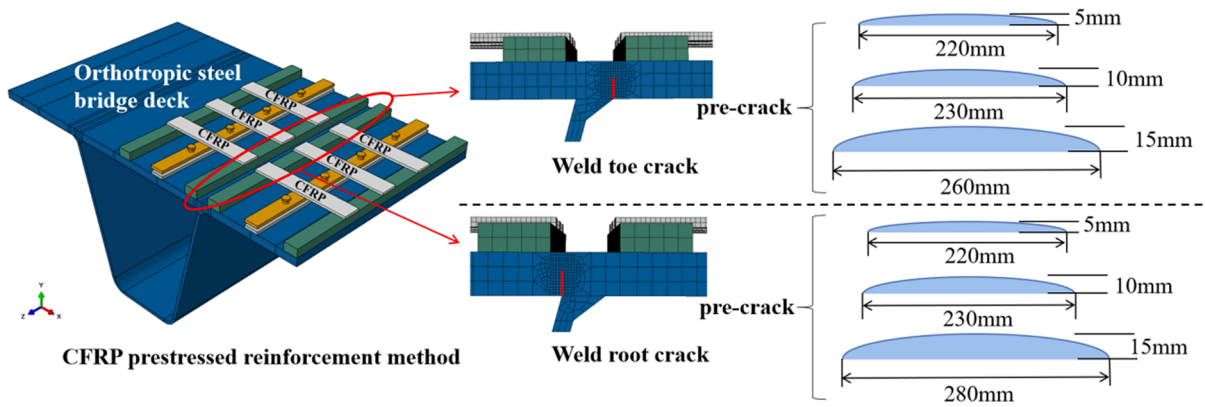


Fig. 18. pre-cracks at the weld toe and root of the OSD reinforced with prestressed CFRP.

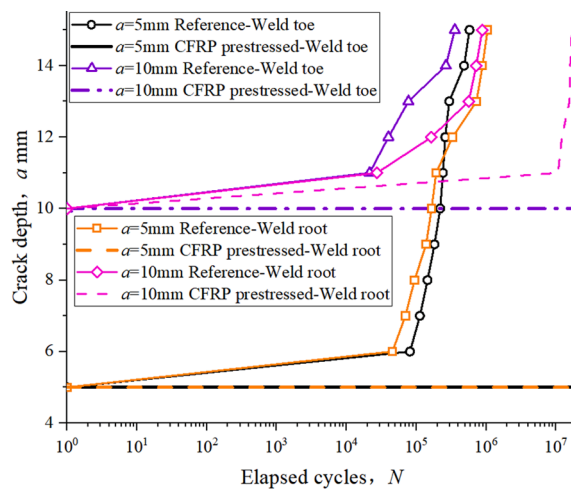


Fig. 19. Numerical simulation results of fatigue crack growth along the depth direction.

Table 9

Fatigue crack growth life ratio in depth direction.

| Cracked area            |          | Weld toe |          |          | Weld root |        |     |
|-------------------------|----------|----------|----------|----------|-----------|--------|-----|
| Pre-crack<br>(mm)       | $a$      | 5        | 10       | 15       | 5         | 10     | 15  |
|                         | $2C$     | 220      | 224      | 256      | 212       | 220    | 264 |
| Crack depth<br>$a$ (mm) | 5        | NAN      | NAN      | NAN      | NAN       | NAN    | NAN |
|                         | 6        | $\infty$ |          |          | $\infty$  |        |     |
|                         | 7        | $\infty$ |          |          | $\infty$  |        |     |
|                         | 8        | $\infty$ |          |          | $\infty$  |        |     |
|                         | 9        | $\infty$ |          |          | $\infty$  |        |     |
|                         | 10       | $\infty$ |          |          | $\infty$  |        |     |
|                         | 11       | $\infty$ | $\infty$ |          | $\infty$  | 392.45 |     |
|                         | 12       | $\infty$ | $\infty$ |          | $\infty$  | 73.56  |     |
|                         | 13       | $\infty$ | $\infty$ |          | $\infty$  | 27.77  |     |
|                         | 14       | $\infty$ | $\infty$ |          | $\infty$  | 22.08  |     |
| 15                      | $\infty$ | $\infty$ |          | $\infty$ | 19.17     |        |     |
| Mean value              |          | $\infty$ | $\infty$ |          | $\infty$  | 107.01 |     |

3. The reinforcement effect of the new CFRP prestressed reinforcement method on the weld toe and root is closely related to the prestress level. When the CFRP prestress makes the stress intensity factor amplitude of the fatigue crack tip less than the fatigue threshold, the fatigue crack stops propagating. After increasing the weight by 13%, the fatigue crack with a depth of less than 1 mm

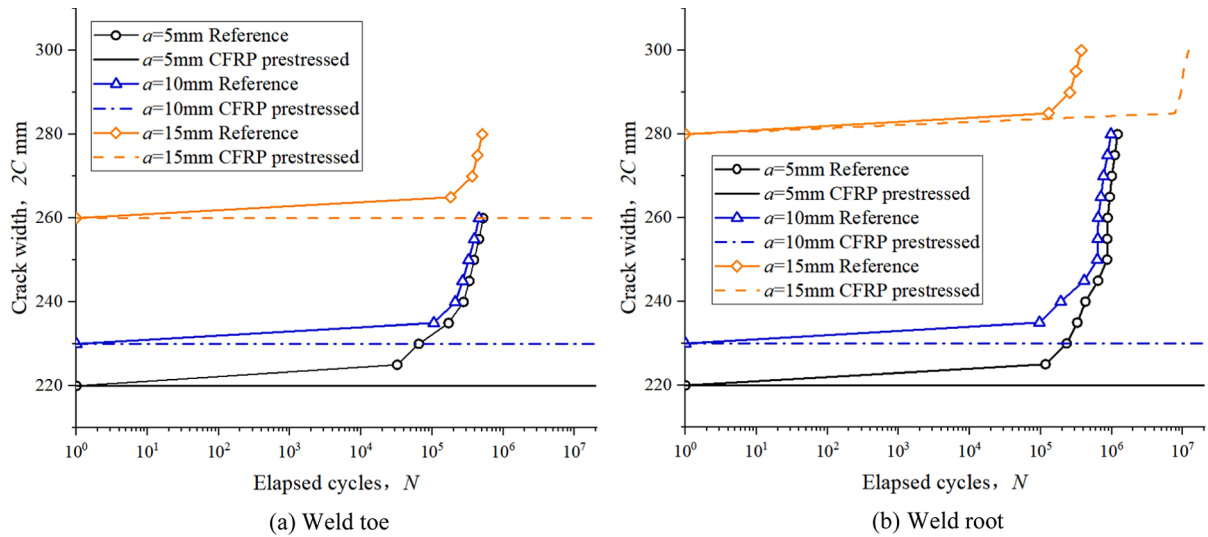


Fig. 20. Numerical simulation results of fatigue crack growth along the width direction. (a)Weld toe. (b)Weld root.

Table 10  
Fatigue crack growth life ratio in width direction.

| Cracked area                   |            | Weld toe |     |     | Weld root |       |       |
|--------------------------------|------------|----------|-----|-----|-----------|-------|-------|
| Pre-crack<br>(mm)              | <i>a</i>   | 5        | 10  | 15  | 5         | 10    | 15    |
|                                | 2 <i>C</i> | 220      | 230 | 260 | 220       | 230   | 280   |
| Crack width<br>2 <i>C</i> (mm) | 220        | NAN      | NAN | NAN | ∞         | NAN   | NAN   |
|                                | 225        |          |     |     | ∞         |       |       |
|                                | 230        |          |     |     | ∞         |       |       |
|                                | 235        | ∞        |     |     | ∞         | ∞     |       |
|                                | 240        | ∞        | ∞   |     | ∞         | ∞     |       |
|                                | 245        | ∞        | ∞   |     | ∞         | ∞     |       |
|                                | 250        | ∞        | ∞   |     | ∞         | ∞     |       |
|                                | 255        | ∞        | ∞   |     | ∞         | ∞     |       |
|                                | 260        | ∞        | ∞   |     | ∞         | ∞     |       |
|                                | 265        | ∞        | ∞   | ∞   | ∞         | ∞     |       |
|                                | 270        | ∞        | ∞   | ∞   | ∞         | ∞     |       |
|                                | 275        | ∞        | ∞   | ∞   | ∞         | ∞     |       |
|                                | 280        | ∞        | ∞   | ∞   | ∞         | ∞     |       |
|                                | 285        | ∞        | ∞   | ∞   | ∞         | ∞     | 60.22 |
| 290                            | ∞          | ∞        | ∞   | ∞   | ∞         | 36.76 |       |
| 295                            | ∞          | ∞        | ∞   | ∞   | ∞         | 32.40 |       |
| 300                            | ∞          | ∞        | ∞   | ∞   | ∞         | 32.26 |       |
| Mean value                     |            | ∞        | ∞   | ∞   | ∞         | ∞     | 40.41 |

at the weld toe stops propagating when the prestress is greater than 280.0 MPa, and the fatigue crack with a depth of less than 1 mm at the weld root stops propagating when the prestress is greater than 560.0 MPa.

- Using 280.0 MPa prestressed CFRP plate to reinforce the OSD can stop the propagation of fatigue cracks with different depths at the weld toe. Using 560.0 MPa prestressed CFRP plate to reinforce the OSD can stop the propagation of fatigue cracks with a depth of less than 5 mm at the weld root and can increase the residual fatigue life of the weld root with a 10 mm deep fatigue crack by 106 times.
- The conclusions of this paper are obtained through the extended finite element numerical simulation verified by experiments. However, in engineering practice, there are often errors, such as material errors and installation errors, which lead to deviations between actual reinforcement effects and theoretical results. Therefore, we will carry out corresponding tests to further verify the proposed new CFRP prestressed reinforcement method in the future.

Declaration of Competing Interest

The authors declare that they have no known competing financial interests or personal relationships that could have appeared to influence the work reported in this paper.

## Data availability

Data will be made available on request.

## Acknowledgments

The authors gratefully acknowledge the financial support provided by the Fundamental Research Funds for the Central Universities, CHD (Grants #300102212514). The calculations were performed by using the HPC Platform at Xi'an Jiaotong University.

## References

- [1] N. van den Berg, H. Xin, M. Veljkovic, Effects of residual stresses on fatigue crack propagation of an orthotropic steel bridge deck, *Mater. Des.* 198 (2021), 109294.
- [2] B. Cheng, X. Ye, X. Cao, D.D. Mbako, Y. Cao, Experimental study on fatigue failure of rib-to-deck welded connections in orthotropic steel bridge decks, *Int. J. Fatigue* 103 (2017) 157–167.
- [3] F. Yan, W. Chen, Z. Lin, Prediction of fatigue life of welded details in cable-stayed orthotropic steel deck bridges, *Eng. Struct.* 127 (2016) 344–358.
- [4] G. Alencar, A. de Jesus, J.G.S. da Silva, R. Calcada, Fatigue cracking of welded railway bridges: A review, *Eng. Fail. Anal.* 104 (2019) 154–176.
- [5] M.H. Kolstein, *Fatigue classification of welded joints in orthotropic steel bridge decks*, 2007.
- [6] B. Ji, R. Liu, C. Chen, H. Maeno, X. Chen, Evaluation on root-deck fatigue of orthotropic steel bridge deck, *J. Constr. Steel Res.* 90 (2013) 174–183.
- [7] W.A. Chun-sheng, Z.H. Mu-sai, T.A. You-ming, Cold maintenance technique and assessment method for orthotropic steel bridge deck, *China J. Highway Transport* 29 (8) (2016) 50.
- [8] J. Liu, T. Guo, D. Feng, Z. Liu, Fatigue performance of rib-to-deck joints strengthened with FRP angles, *J. Bridg. Eng.* 23 (9) (2018) 04018060.
- [9] A. Tabata, Y. Aoki, Y. Takada, Study on improvement of the fatigue durability by filling of mortar in U-shaped rib of orthotropic steel deck, in: *Proceedings of the 5th International Conference on Bridge Maintenance, Safety and Management*, Taylor & Francis, London, 2010, pp. 2799–2805.
- [10] T. Guo, J. Liu, Y. Deng, Z. Zhang, Fatigue performance of orthotropic steel decks with FRP angles: field measurement and numerical analysis, *J. Perform. Constr. Facil* 33 (4) (2019) 04019042.
- [11] Z. Zhu, Z. Xiang, Y.E. Zhou, Fatigue behavior of orthotropic steel bridge stiffened with ultra-high performance concrete layer, *J. Constr. Steel Res.* 157 (2019) 132–142.
- [12] S. Teixeira de Freitas, H. Kolstein, F. Bijlaard, Structural monitoring of a strengthened orthotropic steel bridge deck using strain data, *Struct. Health Monit.* 11 (5) (2012) 558–576.
- [13] S.T. de Freitas, H. Kolstein, F. Bijlaard, Sandwich system for renovation of orthotropic steel bridge decks, *J. Sandw. Struct. Mater.* 13 (3) (2011) 279–301.
- [14] Y. Wang, X. Shao, J. Chen, J. Cao, S. Deng, UHPC-based strengthening technique for orthotropic steel decks with significant fatigue cracking issues, *J. Constr. Steel Res.* 176 (2021), 106393.
- [15] A. Hosseini, E. Ghafoori, M. Motavalli, A. Nussbaumer, X.L. Zhao, Mode I fatigue crack arrest in tensile steel members using prestressed CFRP plates, *Compos. Struct.* 178 (2017) 119–134.
- [16] A. Hosseini, A. Nussbaumer, M. Motavalli, X.L. Zhao, E. Ghafoori, Mixed mode I/II fatigue crack arrest in steel members using prestressed CFRP reinforcement, *Int. J. Fatigue* 127 (2019) 345–361.
- [17] J. Deng, J. Li, M. Zhu, Fatigue behavior of notched steel beams strengthened by a prestressed CFRP plate subjected to wetting/drying cycles, *Compos. B Eng.* 230 (2022), 109491.
- [18] W. Nagy, *Fatigue assessment of orthotropic steel decks based on fracture mechanics (Doctoral dissertation, Ghent University)*, 2017.
- [19] H. Xin, J.A. Correia, M. Veljkovic, Three-dimensional fatigue crack propagation simulation using extended finite element methods for steel grades S355 and S690 considering mean stress effects, *Eng. Struct.* 227 (2021), 111414.
- [20] T. Rabczuk, G. Zi, A. Gerstenberger, W.A. Wall, A new crack tip element for the phantom-node method with arbitrary cohesive cracks, *Int. J. Numer. Meth. Eng.* 75 (5) (2008) 577–599.
- [21] R. Krueger, Virtual crack closure technique: History, approach, and applications, *Appl. Mech. Rev.* 57 (2) (2004) 109–143.
- [22] A. Hobbacher, *Recommendations for fatigue design of welded joints and components*, Vol. 47, Springer International Publishing, Cham, 2016.
- [23] B. Wang, X.Y. Zhou, A. Chen, Probabilistic study on the macro-crack initiation of the rib-to-deck welded joint on orthotropic steel deck, *Int. J. Fatigue* 139 (2020), 105721.
- [24] Y. Zhang, H. Xin, J.A. Correia, Fracture evaluation of ultra-high-performance fiber reinforced concrete (UHPFRC), *Eng. Fail. Anal.* 120 (2021), 105076.